Supporting Information

Biophysical fragment screening of the β_1-adrenergic receptor: Identification of high affinity aryl piperazine leads using structure-based drug design

John A. Christopher,[,†] Jason Brown,[†] Andrew S. Doré,[†] James C. Errey,[†] Markus Koglin,[†], Fiona H. Marshall,[†] David G. Myszka,[‡] Rebecca L. Rich[‡] Christopher G. Tate,[§] Benjamin Tehan,[†] Tony Warne,[§] Miles Congreve.[†]*

[†] Heptares Therapeutics Ltd., BioPark, Welwyn Garden City, Hertfordshire, AL7 3AX, U.K.

[‡] Biosensor Tools LLC, Salt Lake City, Utah 84103 United States.

[§] MRC Laboratory of Molecular Biology, Francis Crick Avenue, Cambridge Biomedical Campus, Cambridge CB2 0QH, U.K.

Table of contents

S2 Table 1: Supplier information and LCMS QC data for fragments **7**-**24.**

S3 ^{1}H and ^{13}C NMR data for compounds **19** and **20**; ^{1}H NMR data for compounds **9**, **21**, **15** and **17**.

S9 Muscarinic M_1-M_4 acetylcholine receptor membrane binding and agonist functional assay details and data for compounds **12, 13, 19, 20**.

S11 Table 2: Data processing, refinement and evaluation statistics.

S13 Table 3: Receptor-ligand interactions and ligand binding pocket dimensions.

S15 Figure 1: Omit maps for the ligands **19** and **20** in the crystal structures.

S16 References

Table 1: Supplier information and LCMS QC data for fragments 7-24.

Fragments **7**−**24** were purchased from ABCR, Acros, Alfa-Aesar, Apollo, Asinex, Chembridge, Fluorochem, Maybridge, Peakdale Molecular, and Sigma-Aldrich as detailed below. The compounds were supplied with purities of >95% as determined by the vendors. LCMS quality control data generated by the authors are detailed below; compounds determined to be < 95% purity by LCMS were additionally analysed by ^{1}H NMR and confirmed to be > 95%.

Compound	Supplier	Supplier ID	MW	LCMS purity[a]	MS data[b] m/z (ESI +)	QC comment
7	Apollo	PC4343	230.2	>98%	231.2	-
8	Sigma-Aldrich	Q1004	213.3[c]	>98%	214.2	-
9	Acros	13082	162.2	93%	163.2	*f*
10	Fluorochem	005906	231.2	>98%	232	-
11	Fluorochem	033323	233.2	>98%	233.2	-
12	Apollo	OR6834	231.1	>98%	231.0, 233.0	-
13	Apollo	OR1481	231.1	>98%	231.0, 233.0	-
14	Fluorochem	9768	231.1	>98%	231.0, 233.0	-
15	Maybridge	AC13696	190.3	94%	191.2	*f*
16	Maybridge	AC13693	190.3	>98%	191.2	-
17	Apollo	PC0865	298.2	91%	299.1	*f*
18	Fluorochem	019027	222.3	95%	223.2	-
19	ABCR	AB153444	201.3[d]	95%	202.2	*g*
20	Alfa-Aeser	H50881	227.3	>98%	228.2	*g*
21	Peakdale	1014191	295.4[e]	93%	296.2	*f*
22	Apollo	OR27760	227.3	>98%	228.2	-
23	Chembridge	9140648	320.5	>98%	321.2	-
24	Asinex	ASN 05542083	302.4	>98%	303.2	-

[a] Data generated by Heptares. [b] LCMS data with electrospray ionisation were generated at Heptares using an Agilent 1260 Infinity LC with Diode Array Detector coupled to an Agilent 6120B Single Quadrupole MS with API-ES source. [c] Supplied as the Maleate salt (free base MW 213.3). [d] Supplied as the dihydrochloride salt (free base MW 201.3). [e] Supplied as the hydrochloride salt (free base MW 295.4). [f] Further analysed by ^{1}H NMR and determined to be > 95% purity, spectroscopic data are below. [g] Further analysed by ^{1}H and ^{13}C NMR prior to crystallography trials, spectroscopic data are below.

^{1}H NMR (d^{6}-DMSO) and ^{13}C NMR (d^{6}-DMSO / D_2O 2:1) data for compound 19.

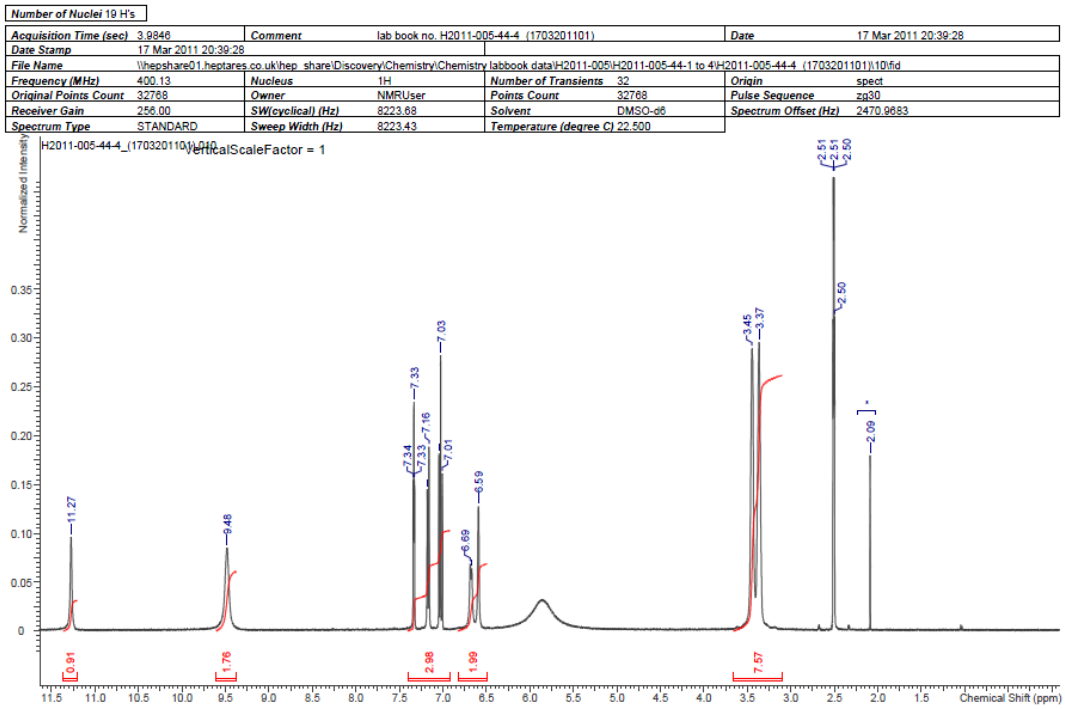

^{1}H NMR (400 MHz, DMSO-d_6) δ ppm 3.37 (br. s, 4 H), 3.45 (br. s, 4 H), 6.59 (br. s, 1 H), 6.68 (d, *J*=6.8 Hz, 1 H), 7.03 (t, *J*=7.9 Hz, 1 H), 7.17 (d, *J*=8.0 Hz, 1 H), 7.33 (t, *J*=2.8 Hz, 1 H), 9.48 (br. s, 2 H), 11.27 (br. s, 1 H).

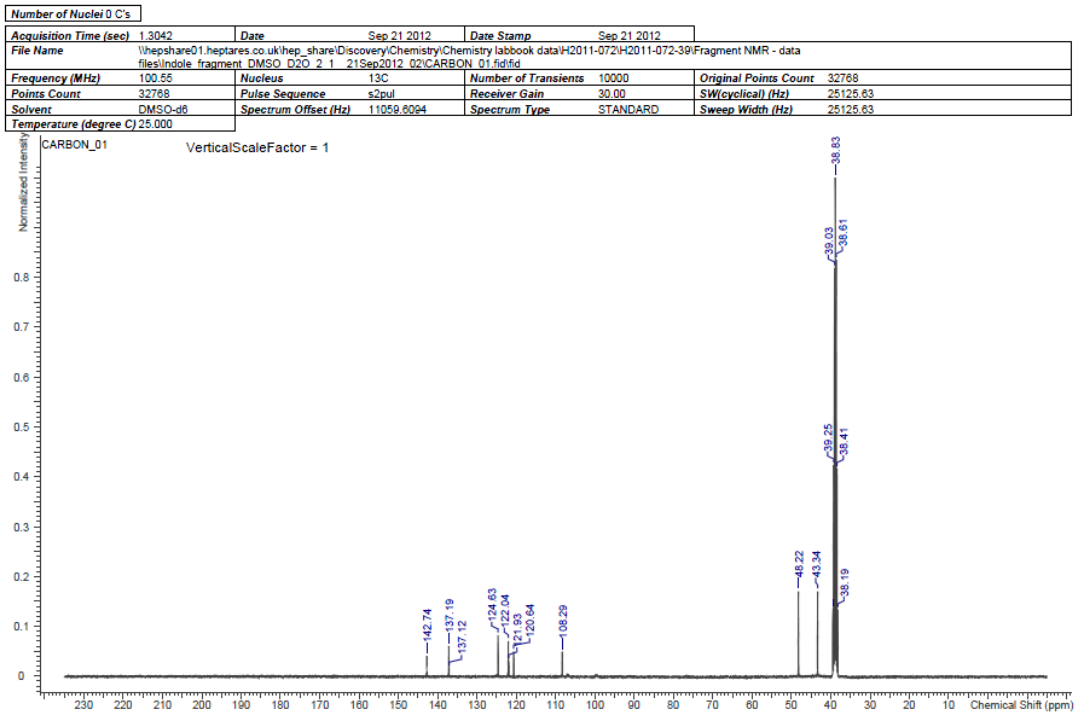

^{13}C NMR (101 MHz, DMSO-d_6 / D_2O 2:1), δ ppm 43.34 (s, 2 C), 48.22 (s, 2 C), 108.29 (s, 1 C), 120.64 (s, 1 C), 121.93 (s, 1 C), 122.04 (s, 1 C), 124.63 (s, 1 C), 137.12 (s, 1 C), 137.19 (s, 1 C), 142.74 (s, 1 C).

^{1}H and ^{13}C NMR (d^{6}-DMSO) data for compound 20.

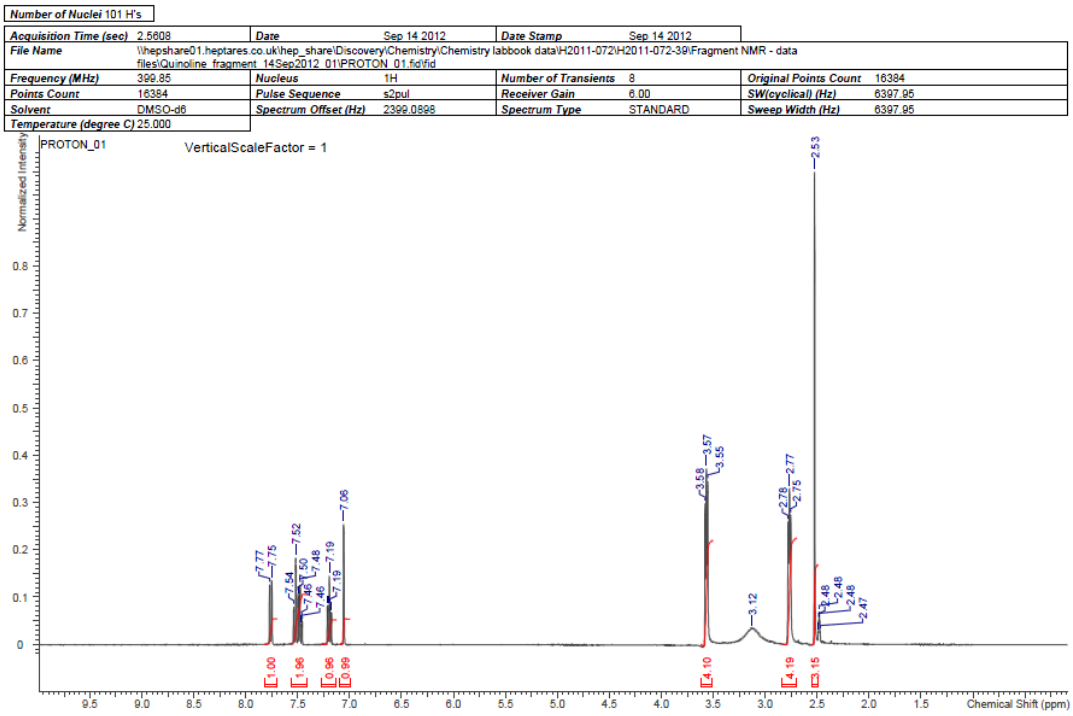

^{1}H NMR (400 MHz, DMSO-d_6) δ ppm 2.53 (s, 3 H), 2.75 - 2.78 (m, 4 H), 3.55 - 3.58 (m, 4 H), 7.06 (s, 1 H), 7.19 (ddd, *J*=8.1, 6.7, 1.6 Hz, 1 H), 7.46 - 7.50 (m, 2 H), 7.76 (d, *J*=8.2 Hz, 1 H).

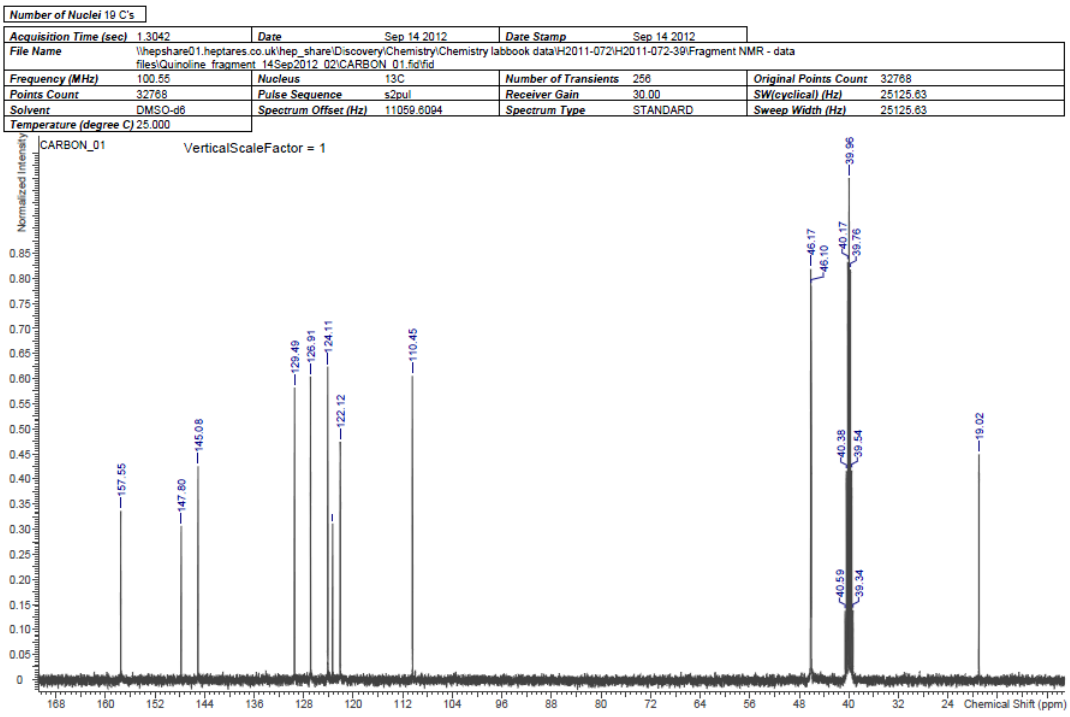

^{13}C NMR (101 MHz, DMSO-d_6) δ ppm 19.02 (s, 1 C), 46.10 (s, 2 C), 46.17 (s, 2 C), 110.45 (s, 1 C), 122.12 (s, 1 C), 123.36 (s, 1 C), 124.11 (s, 1 C), 126.91 (s, 1 C), 129.49 (s, 1 C), 145.08 (s, 1 C), 147.80 (s, 1 C), 157.55 (s, 1 C).

^{1}H NMR data for compounds 9, 15, 17 and 21.

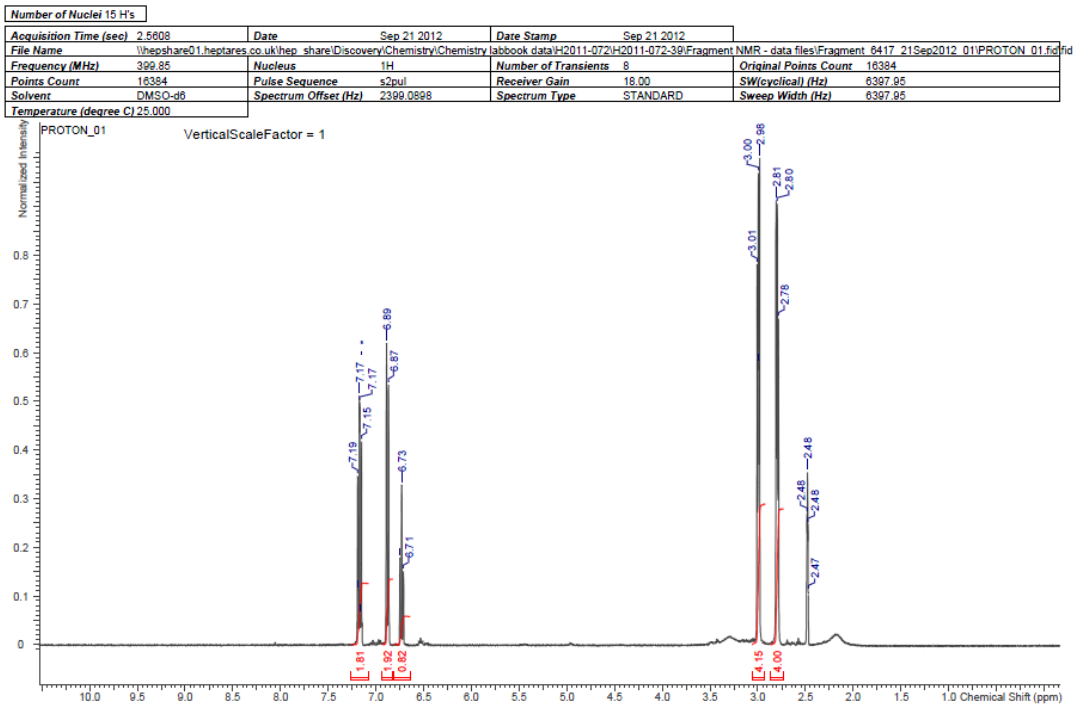

Compound **9**: ^{1}H NMR (400 MHz, DMSO-d_6) δ ppm 2.78 - 2.81 (m, 4 H) 2.98 - 3.01 (m, 4 H) 6.73 (t, *J*=7.4 Hz, 1 H) 6.88 (d, *J*=7.8 Hz, 2 H) 7.15 - 7.19 (m, 2 H)

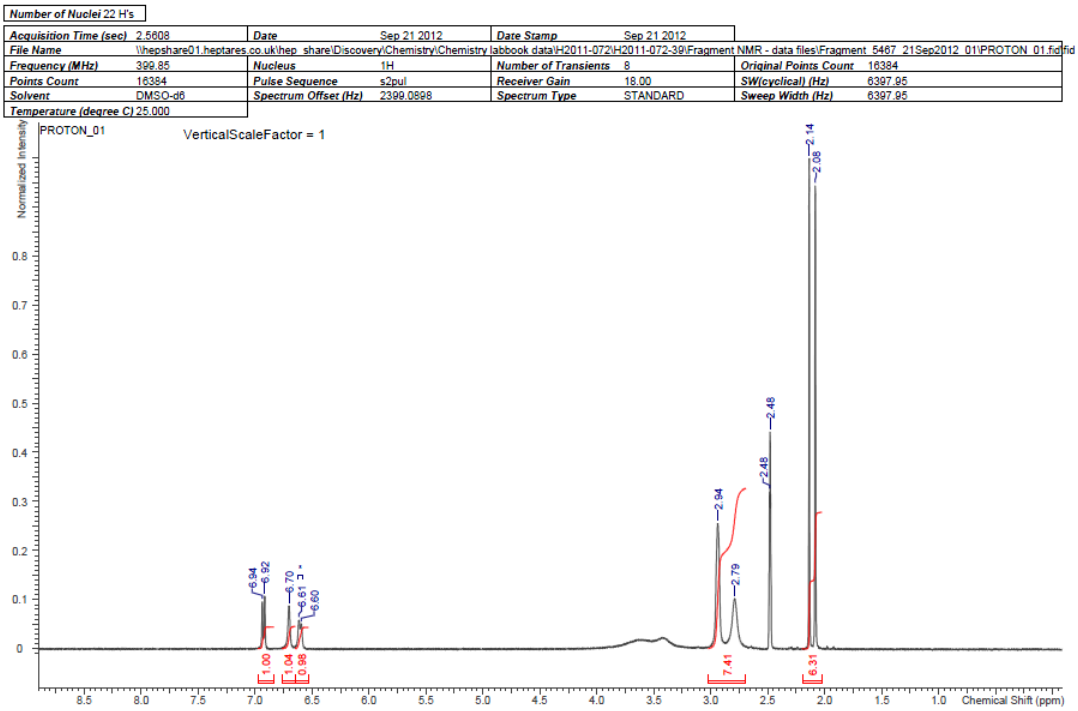

Compound **15**: ^{1}H NMR (400 MHz, DMSO-d_6) δ ppm 2.08 (s, 3 H), 2.14 (s, 3 H), 2.79 (br. s, 4 H), 2.94 (br. s, 4 H), 6.60 (d, *J*=7.4 Hz, 1 H), 6.70 (br. s, 1 H), 6.93 (d, *J*=8.2 Hz, 1 H).

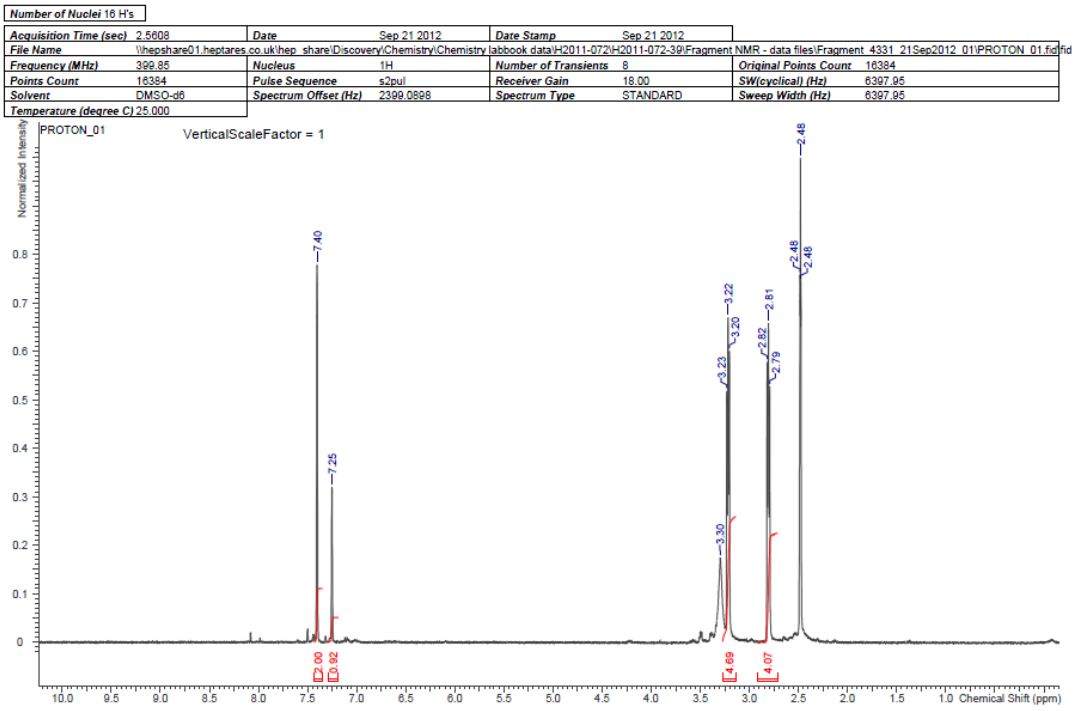

Compound **17**: ^{1}H NMR (400 MHz, DMSO-d_6) δ ppm 2.79 - 2.82 (m, 4 H), 3.20 - 3.24 (m, 4 H), 7.25 (s, 1 H), 7.40 (s, 2 H).

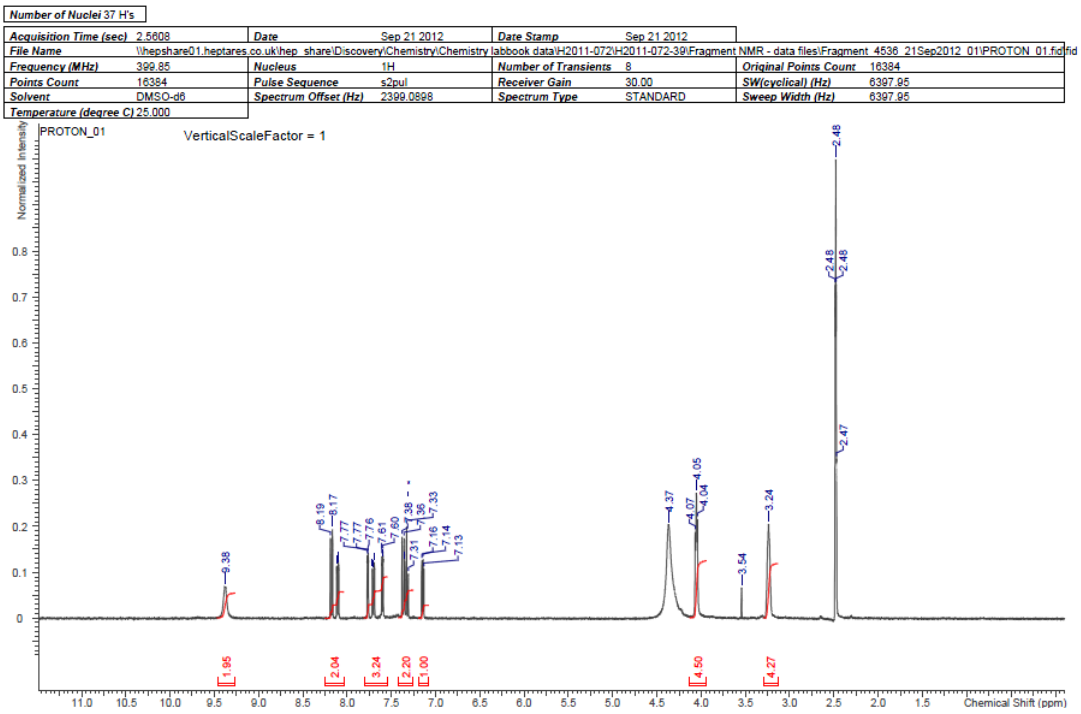

Compound **21**: ^{1}H NMR (400 MHz, DMSO-d_6) δ ppm 3.24 (br. s, 4 H), 4.03 - 4.07 (m, 4 H), 7.15 (dd, *J*=5.1, 3.9 Hz, 1 H), 7.31 – 7.38 (m, 2 H), 7.60 (dd, *J*=5.3, 1.0 Hz, 1 H), 7.70 (dd, *J*=7.8, 1.2 Hz, 1 H), 7.77 (dd, *J*=3.7, 1.0 Hz, 1 H), 8.11 (dd, *J*=7.6, 1.4 Hz, 1 H), 8.18 (d, *J*=9.0 Hz, 1 H), 9.38 (br. s, 2 H, exchangeable).

Muscarinic M_1, M_2, M_3 and M_4 acetylcholine receptor membrane binding and agonist functional assay data for compounds 12, 13, 19, 20.

	pK_i				pEC_{50}				E_{max} (%)			
	M_1	M_2	M_3	M_4	M_1	M_2	M_3	M_4	M_1	M_2	M_3	M_4
12	5.2	5.4	5.1	4.5	< 4.7	< 4.7	< 4.7	< 4.7	< 10	< 10	< 10	< 10
13	4.6	4.5	4.6	< 4.2	< 4.7	< 4.7	< 4.7	< 4.7	< 10	< 10	< 10	16
19	< 4.5	4.5	< 4.5	< 4.2	< 4.7	< 4.7	< 4.7	< 4.7	< 10	< 10	< 10	< 10
20	< 4.5	4.5	4.5	< 4.2	< 4.7	< 4.7	< 4.7	< 4.7	< 10	< 10	< 10	< 10

Muscarinic M_1-M_4 acetylcholine receptor membrane binding assays.

Cell membranes prepared from CHO-K1 cells stably expressing the relevant recombinant muscarinic acetylcholine receptor (supplied by Chantest[1]) were incubated with [^{3}H]-NMS (scopolamine methyl chloride (*N*-Methyl-^{3}H)) in Krebs Ringer pH 7.7 assay buffer in a total assay volume of 0.40 mL. After 60 min incubation at room temperature the reaction was terminated by rapid filtration through GF/B 96-well glass fibre plates using a Tomtec cell harvester. Bound radioactivity was determined through liquid scintillation using Lablogic SafeScint and detected on a microbeta liquid scintillation counter. Competition binding was performed incubating membranes (5, 13, 3 or 5 μg protein / well for M_1-M_4 respectively) with 5 nM concentration of [^{3}H]-NMS and a range of concentrations of the test compound. IC_{50} values were derived from fitting to a four parameter logistic equation in PRISM (GraphPad Software, San Diego, CA, USA). Apparent K_i values were derived using the equation of Cheng and Prusoff.[2] Binding affinities are expressed as pKi values, where $pKi = -\log_{10} Ki$.

Muscarinic M_1-M_4 acetylcholine receptor phospho-ERK1/2 functional assays.

Functional assays were performed using the Alphascreen Surefire phospho-ERK1/2 assay.[3] ERK1/2 phosphorylation is a downstream consequence of both Gq/11 and Gi/o protein coupled receptor activation, making it highly suitable for the assessment of M_1, M_3 (Gq/11 coupled) and M_2, M_4 receptors (Gi/o coupled), rather than using different assay formats for different receptor subtypes. CHO cells

stably expressing the human muscarinic M_1, M_2, M_3 or M_4 receptor were plated (25K / well) onto 96-well tissue culture plates in MEM-alpha + 10% dialysed FBS. Once adhered, cells were serum-starved overnight. Agonist stimulation was performed by the addition of 5 µL agonist to the cells for 5 min (37 °C). Media was removed and 50 µL of lysis buffer added. After 15 min, a 4 µL sample was transferred to 384-well plate and 7 µL of detection mixture added. Plates were incubated for 2 h with gentle agitation in the dark and then read on a PHERAstar plate reader. pEC_{50} and E_{max} figures were calculated from the resulting data for each receptor subtype.

Table 2: Data processing, refinement and evaluation statistics.

	β_1AR-**19**	β_1AR-**20**
Number of crystals	1	1
Space group	$P2_1$	$P2_1$
Cell dimensions *a, b, c* (Å), β (^{o})	89.8, 61.4, 100.8, 108.9	90.0, 60.8, 101.2, 109.2
Data Processing		
Resolution (Å)	61.4 - 2.8	51.3 - 2.7
Rmerge[a]	0.177 (0.647)	0.149 (0.415)
$\langle I/\sigma(I) \rangle$ [a]	6.8 (1.9)	13.4 (1.9)
Completeness (%)[a]	92.5 (90.9)	96.1 (91.2)
Multiplicity[a]	3.3 (2.7)	3.0 (2.0)
Wilson B factor (Å^2)	61.2	59.9
Refinement		
Total number of reflections	23841	27544
Total number of atoms	4998	4952
Number of sodium ions	3	4
Number of waters	35	35
Total number of CHS molecules	4	4
Number of detergent molecules	9	8
R_{work}[b,c]	0.22 (0.278)	0.226 (0.300)
R_{free}[c,d]	0.274 (0.354)	0.266 (0.368)
r.m.s. deviation bonds (Å)	0.009	0.011
r.m.s. deviation angles (^{o})	1.306	1.434
Mean atomic B factor (Å^2)	45.2	48.7
Estimated coordinate error (Å)	0.2	0.21
Ramachandran plot favoured (%)[e]	97.2	97.6

Ramachandran plot outliers (%)[e]	0	0

[a] Values in parentheses are for the highest resolution bin (Å) (β_1AR-**19**, 2.95-2.8; β_1AR-**20**, 2.85-2.7).

[b] Number of reflections used to calculate R_{work} (β_1AR-**19**, 22615 [94.9%];β_1AR-**20**, 26121 [94.9%]).

[c] Values in parentheses are for the highest resolution bin for refinement (Å) (β_1AR-**19**, 2.873–2.80; β_1AR-**20**, 2.77–2.70).

[d] Number of reflections from a randomly selected subset used to calculate R_{free} (β_1AR-**19**, 1214 [5.1%];β_1AR-**20**, 1416 [5.1%]).

[e] Figures obtained using MolProbity.[4]

Table 3: Receptor-ligand interactions and ligand binding pocket dimensions.

Amino acid residue	B-W number	Secondary structure	β_1AR-**19**	β_1AR-**20**	β_1AR-carazolol	β_1AR-cyanopindolol
Trp117	3.28	H3	-	-	v der W	v der W
Thr118	3.29	H3	-	-	-	v der W
Asp121	3.32	H3	Polar	H-bond	H-bond	H-bond
Val122	3.33	H3	v der W	v der W	v der W	v der W
Val125	3.36	H3	-	-	v der W	-
Phe201	-	EL2	v der W	v der W	v der W	v der W
Thr203	-	EL2	-	-	-	Polar
Tyr207	5.38	H5	-	v der W	v der W	-
Ala208	5.39	H5	-	v der W	-	v der W
Ser211	5.42	H5	H-bond	v der W	Polar	H-bond
Ser215	5.46	H5	v der W	v der W	v der W	v der W
Trp303	6.48	H6	v der W	v der W	v der W	v der W
Phe306	6.51	H6	v der W	v der W	v der W	v der W
Phe307	6.52	H6	v der W	v der W	v der W	v der W
Asn310	6.55	H6	v der W	v der W	v der W	H-bond
Asn329	7.39	H7	Polar	Polar	H-bond	H-bond
Tyr333	7.43	H7	-	Polar	v der W	v der W
Binding pocket dimensions: distance Cα Asn329-Ser211 (Å)*			15.8	15.9	15.8	15.9

Amino acid side chain contacts between β_1AR and ligands and dimensions of the ligand binding pocket. Ligand-receptor interactions and ligand binding pocket dimensions have been determined using different monomers which best represent the physiologically relevant conformation as follows: β_1AR-**19**, β_1AR-**20** and β_1AR-cyanopindolol (PDB 2VT4), monomer B; β_1AR-carazolol (PDB 2YCW), monomer A. A 2.8Å upper limit (donor-acceptor separation) was applied to define hydrogen (H) bonds, and an upper limit of 3.9Å was applied to van der Waals interactions. All of the residues listed in the table are identical in the human β_1AR, and we would therefore expect similar modes of ligand binding in the human receptor.

***** The binding pocket dimensions given are in all four cases indicative of the binding of antagonists; the binding of the full agonist isoprenaline results in a contraction of 1Å to 14.8Å.[6]

Abbreviations: B-W number, Ballesteros-Weinstein number;[5] EL2, extracellular loop 2; v der W, van der Waals.

Figure 1. Omit maps for the ligands **19** and **20** in the crystal structures. 2Fo-Fc maps are shown where the ligands were omitted from the phase calculation. (a) **19**, contour level 2.5σ, (b) **20**, contour level 1.0σ.

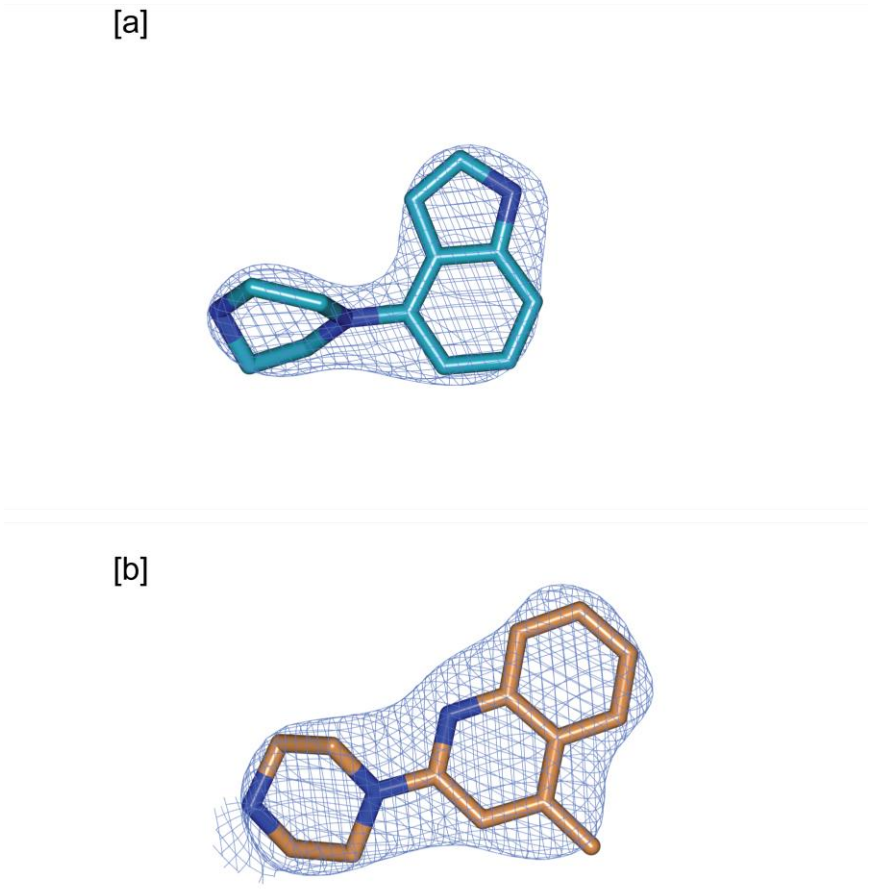

References

1. www.chantest.com

2. Cheng Y.-C.; Prusoff, W. H. Relationship between the inhibition constant (K_i) and the concentration of inhibitor which causes 50 per cent inhibition (I_{50}) of an enzymatic reaction. *Biochem. Pharmacol.* **1973**, *22*, 3099-3108.

3. Crouch, M. F.; Osmond, R. I. W. New Strategies in Drug Discovery for GPCRs: High Throughput Detection of Cellular ERK Phosphorylation. *Comb. Chem. High Throughput Screening* **2008**, *11*, 344-356.

4. Davis, I. W.; Leaver-Fay, A.; Chen, V. B.; Block, J. N.; Kapral, G. J.; Wang, X.; Murray, L. W.; Arendall, W. B., 3rd; Snoeyink, J.; Richardson, J. S.; Richardson, D. C. MolProbity: all-atom contacts and structure validation for proteins and nucleic acids. *Nucleic Acids Res.* **2007**, *35*, W375-383.

5. Ballesteros, J. A.; Weinstein, H. Integrated methods for the construction of three-dimensional models and computational probing of structure-function relations in G protein-coupled receptors. *Methods Neurosci.* **1995**, *25*, 366-428.

6. Warne, T.; Moukhametzianov, M.; Baker, J. G.; Nehmé, R.; Edwards, P. C.; Leslie, A. G. W.; Schertler, G. F. X.; Tate, C. G. The structural basis for agonist and partial agonist action on a β_1-adrenergic receptor. *Nature* **2011**, *469*, 241-244.